Adiabatic treatment of final states in (p,d^*) reactions

B. Gönül* and J. A. Tostevin
Department of Physics, University of Surrey, Guildford, Surrey, GU2 5XH, United Kingdom
(Received 14 December 1995)

The (p,d^*) pickup reaction, leading to spin-singlet and spin-triplet continuum final states of the np system, is treated within the adiabatic approximation. Calculations are carried out for the $^{13}C(p,d^*)$ and $^{13}C(p,d)$ reactions at 35 MeV, leading to the ground and 4.44 MeV states of ^{12}C, for which new data have recently been reported. The np relative energy dependence of the (p,d^*) cross sections and the contributions from triplet and singlet configurations are clarified. We show that, within the adiabatic model, theoretical expectations for the magnitude of the singlet state cross section and of the relative magnitudes of the cross sections for the (p,d) and singlet and triplet (p,d^*) channels are particularly transparent. The calculated adiabatic model cross sections differ by an order of magnitude from recently published calculations and data. We show that vector analyzing power data for the ground state transition could be very valuable in clarifying this disagreement. [S0556-2813(96)01706-2]

PACS number(s): 24.10.−i, 24.50.+g, 25.40.Hs

I. INTRODUCTION

Reactions involving the deuteron, the bound $T=0$, $S=1$ state of the neutron-proton (np) system, play an important part in nuclear structure studies. Theoretically, such data have been invaluable in the assessment of very general theoretical methods for the treatment of three-body and breakup effects in strongly interacting weakly bound systems. The np system, however, also exhibits a virtual $T=1$, $S=0$ state, commonly referred to as the singlet deuteron. The necessity to deal theoretically with the breakup of, and transfer to, such virtual states is likely to become increasingly important for the study of light-neutron-rich systems [1]. In this sense the (p,d^*) reaction provides a prototype for the study of transfer reactions involving virtual state contributions to unbound three-body final states. The (p,d^*) reaction is particularly suited to study these theoretical ideas given our knowledge of the underlying np interaction and the existence, in this case, of the bound deuteron system only 2 MeV in energy from the continuum. The requirement of a consistent description of both the bound and continuum systems is very powerful in assessing the theoretical methods quantitatively.

Reactions involving three-particle final states of a neutron, proton, and third body exhibit strong final state interaction effects between the nucleons, particularly if the np states populated have low relative energy. We refer to such low energy np configurations here by d^*. The major aim of the present work is to quantify the role of the singlet $(S=0)$ spin d^* channel on the (p,d^*) pickup reaction and the accuracy of the adiabatic approximation when the neutron and proton are observed with low relative energy, of order 1 MeV.

Early tentative evidence of singlet deuteron production was reported by many authors, both from incomplete and complete three-body experiments, e.g., [2]. Temmer [3] discussed the possibility of the d^* pickup reaction, suggesting that the state might be observed in a (p,pn) pickup experiment. The possibility of singlet state data suggested the use of such three-body reactions in nuclear spectroscopic studies; however, convenient three-body reaction methods were not then available. In early analyses the final state was assumed to be produced by two-step sequential decay, where the d^* behaves as a single entity for long enough to escape the interaction region. Theoretical treatments reflected this picture via plane wave [4] and distorted wave Born approximation (DWBA) [5] calculations of the singlet and triplet final states. Experimentally, Cohen *et al.* [6] carried out experimental studies of (p,d^*) reactions on odd-neutron targets, showing evidence for singlet deuteron formation. A general conclusion of these earlier works was that, at incident proton energies around 10 MeV, sequential decays through excited target states were significant and complicated the observation of contributions from the np virtual state.

New measurements [7] of neutron pickup to the continuum have recently been reported at 35 MeV incident proton energy. The experimental setup for these data was such as to enhance detection of np pairs in a relative $^1S_0$ state. The data, for a ^{13}C target, include differential cross section data for both the (d,p) and spin singlet $[p,d^*(S=0)]$ channels, leading to both the ground and first 2^+ excited states of ^{12}C. Coupled channels Born approximation (CCBA) calculations, based on the coupled discretized continuum channels (CDCC) method [8] for treating the final states, accompanied the published data for this system [7,10] and appeared to provide a consistent analysis of both the (p,d) and $[p,d^*(S=0)]$ reaction data. Here, we develop a theoretical description of the reactions using the adiabatic approximation [9]. Use of the adiabatic approach makes the connection between the bound and continuum channel transfer reaction calculations particularly transparent. This leads to specific expectations for the relative magnitudes of the cross sections for the two processes based, primarily, upon the elementary properties of the triplet and singlet channel np systems.

At the relative np energies of interest we will assume that the np pair are produced in a relative S state, being either in the $^1S_0$ $(T=1)$ or $^3S_1$ $(T=0)$ states. Since these two spin

* Present and permanent address: Department of Physics, University of Gaziantep, Gaziantep, Turkey.

channels can couple in the final state only as a result of an isovector spin-orbit contribution to the nucleon-nucleus interactions, we can assume that coupling between these spin states is negligible [11]. More generally, with increasing energy, these spin coupling effects will become more important. For example, Al-Khalili *et al.* [12] showed that singlet spin channel coupling has a large effect on the analyzing powers for deuteron scattering at energies in excess of 200 MeV. In that case, however, the coupling proceeds through the isoscalar spin-orbit force and np relative P waves.

The consideration and dominance of low relative continuum energies is well suited to the use of the adiabatic approximation for the treatment of the three-body dynamics in the final state. The adiabatic method was used previously in the study of final state interaction effects in the (^{3}He, pp) system [13]. In this paper we investigate the nature of the np relative energy dependence of the $[p,d^*(S)]$ cross sections and the extent to which the triplet and singlet states contribute to the process. Because of the weak coupling between spin channels, discussed above, the singlet and triplet state contributions to the final state will be analyzed separately.

In the following section we present the formal aspects of the use of the adiabatic approximation in the present context.

II. FORMAL CONSIDERATIONS

We consider the adiabatic formalism for the $^{A+1}X(p,d)^AX$ and $^{A+1}X[p,d^*(S)]^AX$ reactions leading to bound and unbound S-wave np pairs. It is important for the present work to make clear the essential differences in the calculations for the two systems and so they are developed in some detail within a common notation. We will evaluate the transition amplitudes for the processes in a zero-range approximation. While this will affect the deduced values of the spectroscopic factors for the transferred neutron, these can be fixed by reference to the available (p,d) data. The relative magnitudes of the bound and continuum amplitudes, of primary interest here, will be accurately described.

A. Transition amplitudes

Since the coupling of the singlet ($^1S_0$) and triplet ($^3S_1$) continuum np states is negligible, the transition amplitudes for singlet and triplet processes can be considered separately. Thus, the amplitude for neutron pickup, to form an np pair with spin S and relative energy ε_r, is

$$T^S_{fi}(\varepsilon_r)=\langle \Psi^{(-)}_{S\varepsilon_r}(\vec{r},\vec{R})|V^S_{np}|\Phi_{lj}(\vec{r}_n)\chi^{(+)}_p(\vec{r}_p)\rangle, \qquad (1)$$

where V^S_{np} is the np interaction appropriate to spin channel S and where we have denoted the np center of mass (c.m.) and relative coordinates by $\vec{R}$ and $\vec{r}$, respectively. Here Φ_{lj} is the transferred neutron bound state and $\chi^{(+)}_{\rm p}$, the incident proton distorted wave, describes proton elastic scattering from the target. The vectors $\vec{r}_n$ and $\vec{r}_p$ are the positions of the transferred neutron with respect to the A particle core and of the proton relative to the $A+1$ system. For clarity we will not show the transferred neutron spectroscopic factor or any spin projection labels explicitly.

In Eq. (1), $\Psi^{(-)}_{S\varepsilon_r}(\vec{r},\vec{R})$, the three-body wave function for the $n+p+$residual nucleus system, can be evaluated from the corresponding $\Psi^{(+)}_{S\varepsilon_r}(\vec{r},\vec{R})$, being the solution of the Schrödinger equation, for total energy E,

$$[E-H_{np}-T_R-V_n(\vec{r},\vec{R})-V_p(\vec{r},\vec{R})]\Psi^{(+)}_{S\varepsilon_r}(\vec{r},\vec{R})=0. \qquad (2)$$

Here T_R is the np c.m. kinetic energy operator, $V_n(\vec{r},\vec{R})$ and $V_p(\vec{r},\vec{R})$ are the nucleon-residual nucleus optical potentials, and H_{np} is the np relative motion Hamiltonian. Since the np interaction is short ranged, an accurate evaluation of T_{fi} requires that the final state three-body wave functions $\Psi^{(-)}_{S\varepsilon_r}(\vec{r},\vec{R})$ be calculated accurately only in the neighborhood of $|\vec{r}|=0$, i.e., $|\vec{r}|\approx$ range of V_{np}.

The cross section (in the c.m. frame) for neutron pickup to an np pair, with spin S and relative energy ε_r, is given by [14]

$$d^3\sigma(p,d^*)_S=\frac{\mu_i\mu_f}{(2\pi\hbar^2)^2}\frac{k_f}{k_i}|T^S_{fi}(\varepsilon_r)|^2\left[\frac{\mu_r\hbar k_r}{(2\pi\hbar)^3}\right]d\varepsilon_r d\Omega_r d\Omega_f, \qquad (3)$$

where $d\Omega_r\equiv d\hat{k}_r$ and $d\Omega_f\equiv d\hat{k}_f$ are the elements of the solid angle for the asymptotic relative and center of mass momenta of the np pair. In the above the final state c.m. and relative motion wave numbers, k_f, k_r, and ε_r are such that

$$E=E_f+\varepsilon_r=\frac{\hbar^2k_f^2}{2\mu_f}+\frac{\hbar^2k_r^2}{2\mu_r}, \qquad (4)$$

with μ_f and μ_r the c.m. and relative motion reduced masses. The normalization of Eq. (3) implies that all scattering wave functions in $T^S_{fi}(\varepsilon_r)$ have incident plane waves $N\exp(i\vec{K}\cdot\vec{R})$ with $N=1$. Also, in Eq. (3), we do not show explicitly the required spin sums and averages, over target and projectile fragment spin projections, which are carried out in the full spin-dependent calculations.

For the (p,d) reaction then of course $S=1$ and

$$d\sigma(p,d)=\frac{\mu_i\mu_f}{(2\pi\hbar^2)^2}\frac{\widetilde{k}_f}{k_i}|T_{fi}(p,d)|^2d\Omega_f, \qquad (5)$$

where now

$$T_{fi}(p,d)=\langle\Psi^{(-)}_d(\vec{r},\vec{R})|V^{S=1}_{np}|\Phi_{lj}(\vec{r}_n)\chi^{(+)}_p(\vec{r}_p)\rangle. \qquad (6)$$

For the description of the final state one now solves the three-body equation

$$[E-H_{np}-T_R-V_n(\vec{r},\vec{R})-V_p(\vec{r},\vec{R})]\Psi^{(+)}_d(\vec{r},\vec{R})=0, \qquad (7)$$

where the energy-momentum relations are

$$E=\widetilde{E}_f-\varepsilon_d=\frac{\hbar^2\widetilde{k}_f^2}{2\mu_f}-\varepsilon_d. \qquad (8)$$

B. Adiabatic approximation

We solve Eqs. (2) and (7) for the np continuum and deuteron, respectively, in the adiabatic approximation. Thus, as-

suming that the np relative energies of importance are small in relation to E_f and $\widetilde{E}_f$, we replace H_{np} by the np relative energy ε_r and deuteron binding energy $-\varepsilon_d$, respectively, to guarantee the correct asymptotic boundary conditions. Thus

$$\Psi^{(+)}_{S\varepsilon_r}(\vec{r},\vec{R}) \approx \Psi^{\rm ad}_{S\varepsilon_r}(\vec{r},\vec{R}) = \chi^{\rm ad}_{S\varepsilon_r}(\vec{r},\vec{R})\,\phi^S_{\varepsilon_r}(\vec{r}), \tag{9}$$

where $\phi^S_{\varepsilon_r}(\vec{r})$ is a spin S np scattering state with energy ε_r, normalized such that $\phi^S_{\varepsilon_r}(\vec{r}) = \exp(i\vec{k}_r\cdot\vec{r}) + \cdots$, and

$$\Psi^{(+)}_d(\vec{r},\vec{R}) \approx \Psi^{\rm ad}_d(\vec{r},\vec{R}) = \chi^{\rm ad}_d(\vec{r},\vec{R})\,\phi_d(\vec{r}), \tag{10}$$

with $\phi_d(\vec{r})$ the deuteron ground state wave function. The functions $\chi^{\rm ad}$ in Eqs. (9) and (10) satisfy the equations

$$[E_f - T_R - V_n(\vec{r},\vec{R}) - V_p(\vec{r},\vec{R})]\chi^{\rm ad}_{S\varepsilon_r}(\vec{r},\vec{R}) = 0, \tag{11}$$

$$[\widetilde{E}_f - T_R - V_n(\vec{r},\vec{R}) - V_p(\vec{r},\vec{R})]\chi^{\rm ad}_d(\vec{r},\vec{R}) = 0, \tag{12}$$

which now depend only parametrically upon $\vec{r}$. These can be solved for each $\vec{r}$ and, for Eq. (11), for each value of $E_f = E - \varepsilon_r$, over the required range of relative energies in the np final state.

It should be noted that these equations for the np c.m. distortion in the continuum and deuteron channels differ only in the center of mass energy available and, in the case of the singlet continuum, the absence of spin-orbit interaction effects. To the extent that these effects are small, i.e., that for reasonably large E, then $E_f = E - \varepsilon_r \approx E + \varepsilon_d = \widetilde{E}_f$, provided the energy range of the np spectrum is limited and that the spin dependence is weak, the wave functions describing the center of mass motions of the continuum np and bound deuteron systems will be very closely related. It follows that in the adiabatic approximation the required transition amplitudes are

$$T^S_{\rm ad}(\varepsilon_r) = \langle \chi^{\rm ad}_{S\varepsilon_r}(\vec{r},\vec{R})\,\phi^S_{\varepsilon_r}(\vec{r}) | V^S_{np} | \Phi_{lj}(\vec{r}_n)\chi^{(+)}_p(\vec{r}_p)\rangle, \tag{13}$$

$$T_{\rm ad}(p,d) = \langle \chi^{\rm ad}_d(\vec{r},\vec{R})\,\phi_d(\vec{r}) | V^{S=1}_{np} | \Phi_{lj}(\vec{r}_n)\chi^{(+)}_p(\vec{r}_p)\rangle. \tag{14}$$

Although quite general, Eqs. (11) and (12) are solved here assuming that breakup is to np relative S states only. The details of the resulting partial wave expansions and solution of the equations can be found in Sec. III of Ref. [15] in this case.

To make clearer the similarity of the (p,d) and (p,d^*) calculations it is convenient to include the $(2\pi)^{-3}$ factor, appearing in the cross section expression, Eq. (3), within the np continuum states in the transition amplitude. Thus we write

$$d^3\sigma(p,d^*)_S = \frac{\mu_i\mu_f}{(2\pi\hbar^2)^2}\,\frac{k_f}{k_i}|\widetilde{T}^S_{\rm ad}(\varepsilon_r)|^2\rho(\varepsilon_r)d\varepsilon_r d\Omega_r d\Omega_f, \tag{15}$$

where $\rho(\varepsilon_r) = \mu_r\hbar k_r/\hbar^3$ is the density of states factor. The transition amplitude is now

$$\widetilde{T}^S_{\rm ad}(\varepsilon_r) = \langle \chi^{\rm ad}_{S\varepsilon_r}(\vec{r},\vec{R})\,\widetilde{\phi}^S_{\varepsilon_r}(\vec{r}) | V^S_{np} | \Phi_{lj}(\vec{r}_n)\chi^{(+)}_p(\vec{r}_p)\rangle, \tag{16}$$

with the np continuum state

$$\widetilde{\phi}^S_{\varepsilon_r}(\vec{r}) = \sum_{lm} e^{i\delta^S_l(\varepsilon_r)} u^S_l(r) Y_{lm}(\hat{r}) Y^*_{lm}(\hat{k}_r) \tag{17}$$

and where asymptotically

$$u^S_l(r) \to \left(\frac{2}{\pi}\right)^{1/2} \frac{i^l \sin[k_r r - l\pi/2 + \delta^S_l(\varepsilon_r)]}{k_r r}. \tag{18}$$

For the deuteron

$$\phi_d(\vec{r}) = u_0(r) Y_{00}(\hat{r}). \tag{19}$$

C. Zero-range approximation

In calculating the transfer amplitudes, Eqs. (14) and (16), we make use of the zero-range approximation. Thus for the continuum final state we replace

$$V^S_{np}(r)\chi^{\rm ad}_{S\varepsilon_r}(\vec{r},\vec{R})\widetilde{\phi}^S_{\varepsilon_r}(\vec{r}) \approx D_0(S,\varepsilon_r) e^{i\delta^S_0(\varepsilon_r)} Y^*_{00}(\hat{k}_r) \times \chi^{\rm ad}_{S\varepsilon_r}(\vec{r}=0,\vec{R})\,\delta(\vec{r}), \tag{20}$$

with strength parameter

$$D_0(S,\varepsilon_r) = \int d\vec{r} V^S_{np}(r) u^S_0(r) Y_{00}(\hat{r}) = \sqrt{4\pi}\int dr r^2 V^S_{np}(r) u^S_0(r). \tag{21}$$

For the deuteron case, then

$$V^{S=1}_{np}(r)\chi^{\rm ad}_d(\vec{r},\vec{R})\phi_d(\vec{r}) \approx D_0(p,d)\chi^{\rm ad}_d(\vec{r}=0,\vec{R})\,\delta(\vec{r}), \tag{22}$$

with

$$D_0(p,d) = \sqrt{4\pi}\int dr r^2 V^{S=1}_{np}(r) u_0(r). \tag{23}$$

In the zero-range limit only the coincidence breakup wave functions $\chi^{\rm ad}_d(\vec{r}=0,\vec{R})$ and $\chi^{\rm ad}_{S\varepsilon_r}(\vec{r}=0,\vec{R})$ are required. These now satisfy distorted-wave-like equations, Eqs. (11) and (12), but where the distorting potentials are the sum of the neutron and proton optical potentials at coincidence.

It follows that

$$\widetilde{T}^S_{\rm ad}(\varepsilon_r) = D_0(S,\varepsilon_r) e^{-i\delta^S_0(\varepsilon_r)} Y_{00}(\hat{k}_r) M^S_{\rm ad}(\varepsilon_r) = D_0(S,\varepsilon_r) e^{-i\delta^S_0(\varepsilon_r)} Y_{00}(\hat{k}_r) \times \langle \chi^{\rm ad}_{S\varepsilon_r}(\vec{r}=0,\vec{R}) | \Phi_{lj}(\vec{R})\chi^{(+)}_p(\gamma\vec{R})\rangle, \tag{24}$$

$$T_{\rm ad}(p,d) = D_0(p,d) M_{\rm ad}(p,d) = D_0(p,d)\langle \chi^{\rm ad}_d(\vec{r}=0,\vec{R}) | \Phi_{lj}(\vec{R})\chi^{(+)}_p(\gamma\vec{R})\rangle, \tag{25}$$

with $\gamma=A/(A+1)$. Finally therefore

$$d^3\sigma(p,d^*)_S=\frac{\mu_i\mu_f}{(2\pi\hbar^2)^2}\frac{k_f}{k_i}\frac{D_0^2(S,\varepsilon_r)}{4\pi}|M_{\rm ad}^S(\varepsilon_r)|^2 \times\rho(\varepsilon_r)d\varepsilon_r d\Omega_r d\Omega_f. \quad (26)$$

Upon carrying out the integration over all relative momentum directions,

$$\frac{d^2\sigma(p,d^*)_S}{d\Omega_f d\varepsilon_r}=\frac{\mu_i\mu_f}{(2\pi\hbar^2)^2}\frac{k_f}{k_i}D_0^2(S,\varepsilon_r)|M_{\rm ad}^S(\varepsilon_r)|^2\rho(\varepsilon_r), \quad (27)$$

and over a specified range of detected np relative energies $0\leq\varepsilon_r\leq\varepsilon_r^{\max}$, dictated by experimental conditions, the single differential cross for the emergence of a spin-S S-state np pair is

$$\frac{d\sigma(p,d^*)_S}{d\Omega_f}=\int_0^{\varepsilon_r^{\max}}\frac{d^2\sigma(p,d^*)_S}{d\Omega_f d\varepsilon_r}d\varepsilon_r =\frac{\mu_i\mu_f}{(2\pi\hbar^2)^2}\frac{1}{k_i}\int_0^{\varepsilon_r^{\max}}k_f D_0^2(S,\varepsilon_r)|M_{\rm ad}^S(\varepsilon_r)|^2 \times\rho(\varepsilon_r)d\varepsilon_r. \quad (28)$$

For the (p,d) reaction, we obtain the more familiar result

$$\frac{d\sigma(p,d)}{d\Omega_f}=\frac{\mu_i\mu_f}{(2\pi\hbar^2)^2}\frac{\widetilde{k}_f}{k_i}D_0^2(p,d)|M_{\rm ad}(p,d)|^2. \quad (29)$$

To compare calculations of the $[p,d^*(S)]$ process against any set of measured angular distributions it is essential therefore to establish the range of relative energies, $0\leq\varepsilon_r\leq\varepsilon_r^{\max}$, detected, which enter as the limits of the integral over np configurations in Eq. (28). We first investigate, more generally, the theoretically expected relative magnitudes of the singlet and triplet $[p,d^*(S)]$ and (p,d) cross sections as a function of the maximum detected energy $\varepsilon_r^{\max}$.

III. ESTIMATES OF CROSS SECTIONS

We first estimate the singlet and triplet (p,d^*) cross sections relative to those of the (p,d) reaction for the same incident energy and neutron transfer. Since Eqs. (28) and (29) are written without explicit reference to spin quantum numbers, the triplet and singlet channel expressions will need to multiplied by $(2S+1)$ in such a comparison. This is of course exact in the absence of the spin dependence arising from the np-target interactions in the final state. The full spin dependence is included exactly in the calculations presented in the next section.

The ε_r dependence in the integrand of the differential cross section, Eq. (28), originates from four terms: the final state wave number k_f, the zero-range constant $D_0(S,\varepsilon_r)$, the density of states factor $\rho(\varepsilon_r)$, and the adiabatic wave function in $M_{\rm ad}^S(\varepsilon_r)$. All are included in the full calculations. In estimating the cross sections, however, for reasonably large energy E ($=35$ MeV for the data of interest here) and a limited range of np relative energies $0\leq\varepsilon_r\leq\varepsilon_r^{\max}$ (≈1 MeV here) the value of k_f will vary very little over the relative energy interval and can be removed from the integral as $\overline{k_f}$, where $\overline{k_f}\approx\widetilde{k}_f$, is appropriate to the relative energy interval. Also, since the dependence of the amplitudes $M_{\rm ad}^S(\varepsilon_r)$ on ε_r is through the energy value $E_f=E-\varepsilon_r$ in the equation for the adiabatic wave function, Eq. (11), then for a narrow range of ε_r the matrix element will also have only weak dependence on the relative energy. We will therefore write

$$\frac{d\sigma(p,d^*)_S}{d\Omega_f}\approx\frac{\mu_i\mu_f}{(2\pi\hbar^2)^2}\frac{\overline{k_f}}{k_i}|M_{\rm ad}^S(\overline{\varepsilon_r})|^2 \times\int_0^{\varepsilon_r^{\max}}D_0^2(S,\varepsilon_r)\rho(\varepsilon_r)d\varepsilon_r, \quad (30)$$

with $\overline{\varepsilon_r}$ a representative relative energy. Moreover, as was noted earlier, to the extent that the continuum and deuteron channel c.m. energies are very similar, $E_f=E-\varepsilon_r\approx E+\varepsilon_d=\widetilde{E}_f$, and that the final state spin-dependence is weak, the wave functions describing the center of mass motions of both the singlet and triplet continuum and bound deuteron systems will be very similar. Consequently for estimation purposes we can assume $|M_{\rm ad}^S(\overline{\varepsilon_r})|^2\approx|M_{\rm ad}(p,d)|^2$. In this limit the relative magnitudes of the (p,d) and $[p,d^*(S)]$ cross sections will be essentially determined by $3D_0^2(p,d)$ (due to the triplet final state) for the (p,d) reaction and $(2S+1)\overline{D_0^2}(S,\varepsilon_r^{\max})$ for the $[p,d^*(S)]$ reaction, where

$$\overline{D_0^2}(S,\varepsilon_r^{\max})=\int_0^{\varepsilon_r^{\max}}D_0^2(S,\varepsilon_r)\rho(\varepsilon_r)d\varepsilon_r. \quad (31)$$

In this limit, the calculation now takes the form of a single DWBA calculation, with an effective zero-range strength parameter, but with a specific theoretical choice for the final state distorting potentials, namely, the adiabatic potential [9], the sum of the n- and p-residual nucleus interactions at coincidence.

The singlet S-wave scattering states entering $D_0(S,\varepsilon_r)$, Eq. (21), are calculated from both the original Reid soft-core [16] and more recent Nijmegan [17] versions of the $^1S_0$ np interaction. In the spin triplet states we assume the Hulthen potential of Ref. [18] which reproduces the deuteron binding energy and low energy $^3S_1$ phase shifts, but assuming the state is uncoupled to the $^3D_1$ channel. The calculated $^1S_0$ and $^3S_1$ zero-range transfer strengths $D_0^2(S,\varepsilon_r)\rho(\varepsilon_r)$ are presented in Fig. 1 over the relative energy interval $0\leq\varepsilon_r\leq1.5$ MeV. The curves are scaled by $(2S+1)$, as discussed above. The dashed curve shows the result for the $^1S_0$ channel calculated using the Reid soft-core interaction. The solid curve uses the Nijmegan potential, which changes the magnitude of the singlet state amplitude significantly over the entire energy range. Our subsequent calculations use the latter more recent parametrization. The dot-dashed curve is the calculated $^3S_1$ channel strength. The sharp rise and the dominant singlet state strength at small relative energies reflects the S-wave virtual state. By contrast the broader contribution from the triplet state increases at larger relative energies. The results on the presented energy range agree to

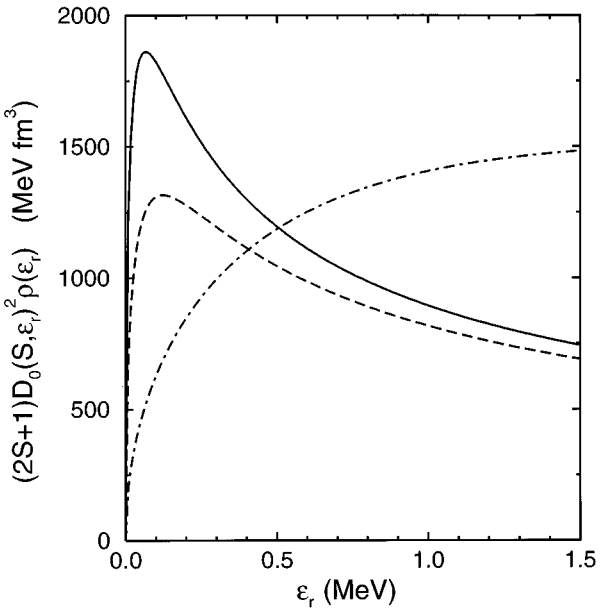

FIG. 1. Calculated zero-range transfer strengths $(2S+1)D_0^2(S,\varepsilon_r)\rho(\varepsilon_r)$ over the np relative energy interval to 1.5 MeV. The $^1S_0$ terms are shown by the dashed and solid curves for the Reid soft-core and Nijmegan potentials, respectively. The dot-dashed curve is the $^3S_1$ strength.

better than 5% (singlet) and 2% (triplet) with those calculated from the Watson-Migdal factor, which, with our normalizations, reads

$$D_0^2(S,\varepsilon_r)\rho(\varepsilon_r)\approx\left[2\sqrt{2}\left(\frac{\hbar^2}{2\mu_r}\right)\left(\frac{\sin\delta_0^S(\varepsilon_r)}{k_r}\right)\right]^2\rho(\varepsilon_r). \tag{32}$$

There are more significant deviations from the forms of Kolltveit and Nagatani [5]. The relationship of theirs and the present work gives

$$D_0^2(S,\varepsilon_r)\rho(\varepsilon_r)\approx\left[2\sqrt{2}\left(\frac{\hbar^2}{2\mu_r}\right)\right]^2\frac{a_S^2}{k_r^2a_S^2+(1-k_r^2a_Sr_S)^2}\rho(\varepsilon_r), \tag{33}$$

where the singlet and triplet scattering lengths and effective range parameters were $a_0=-23.7$ fm, $r_0=2.6$ fm, $a_1=5.38$ fm, and $r_1=1.7$ fm.

The calculated transfer strengths $(2S+1)\overline{D_0^2}(S,\varepsilon_r^{\max})$ are presented in Table I for $\varepsilon_r^{\max}$ values from 0.1 to 1.5 MeV. Also shown is the ratio of the singlet d^* to the deuteron $[3D_0^2(p,d)]$ transfer strengths and the ratio of the expected singlet to triplet d^* final state contributions, expressed as a percentage of the total continuum transfer cross section on the interval $0\leqslant\varepsilon_r\leqslant\varepsilon_r^{\max}$. For the Hulthen potential used [18], $D_0(p,d)=-125.0$ MeV fm$^{3/2}$ or $D_0^2(p,d)=15625$ MeV^2 fm^3. The estimated (p,d) to $[p,d^*(S=0)]$ reaction cross section ratios are shown in the fourth column of the table and depend sensitively on the detected relative motion phase space, as do the fractions of singlet and triplet state continuum strengths, as is evident from Fig. 1. For $\varepsilon_r^{\max}=1.0$ MeV, however, we calculate a factor of 37 difference between the (p,d) and $[p,d^*(S=0)]$ cross sections and approximately equal singlet and triplet channel np contributions.

IV. RESULTS OF FULL ADIABATIC MODEL CALCULATIONS

We calculate the ^{13}C$(p,d)^{12}$C and ^{13}C$(p,d^*)^{12}$C single nucleon transfer reactions leading to the 0^+ ground state ($p_{1/2}$ neutron transfer) and first excited 2^+ ($E_x=4.44$ MeV) state ($p_{3/2}$ neutron transfer) of ^{12}C. We perform zero-range calculations, Eqs. (28) and (29), using a modified version of the program TWOFNR [19]. The radial integrals are carried out from 0 to 20 fm in steps of 0.1 fm. The maximum number of partial waves used was 30 for both the entrance and exit channels. The program has been modified so that the calculated adiabatic radial wave functions can be read in. The separation energy prescription is used for the bound state neutron wave functions in a real Woods-Saxon well. The radius and diffuseness parameters of the bound state potential are 1.25 fm and 0.65 fm, respectively. The bound neutron spin-orbit force is fixed at 6.0 MeV. In the three-body adiabatic model calculations of the deuteron- and np-^{12}C wave functions, Eqs. (11) and (12), we make use of the global optical potential parameter set of Bechetti and Greenlees [20] evaluated at half the final state c.m. energy $(E_f/2)$. The spin-orbit interactions are included and contribute to the $S=1$ channels. The entrance channel proton optical potential parameters are taken from [21], as are those of the deuteron optical potential used in the distorted wave Born approximation calculations for the ^{13}C$(p,d)^{12}$C system which are presented for comparison purposes in Figs. 2 and 3.

TABLE I. Calculated transfer strengths $(2S+1)\overline{D_0^2}(S,\varepsilon_r^{\max})$, ratio of the singlet d^* and deuteron transfer strengths, and percentage singlet state contributions, for $\varepsilon_r^{\max}$ values from 0.1 to 1.5 MeV.

$\varepsilon_r^{\max}$ (MeV)	$\overline{D_0^2}(S=0,\varepsilon_r^{\max})$ (MeV^2 fm^3)	$3\overline{D_0^2}(S=1,\varepsilon_r^{\max})$ (MeV^2 fm^3)	$3D_0^2(p,d)/\overline{D_0^2}(S=0,\varepsilon_r^{\max})$	Singlet (%)
0.1	171.9	44.0	272.6	79.7
0.3	494.2	212.0	94.8	70.0
0.5	754.4	432.2	62.1	63.6
0.7	976.9	682.2	48.0	59.0
1.0	1263.2	1095.2	37.1	53.6
1.5	1671.2	1816.6	28.0	47.9

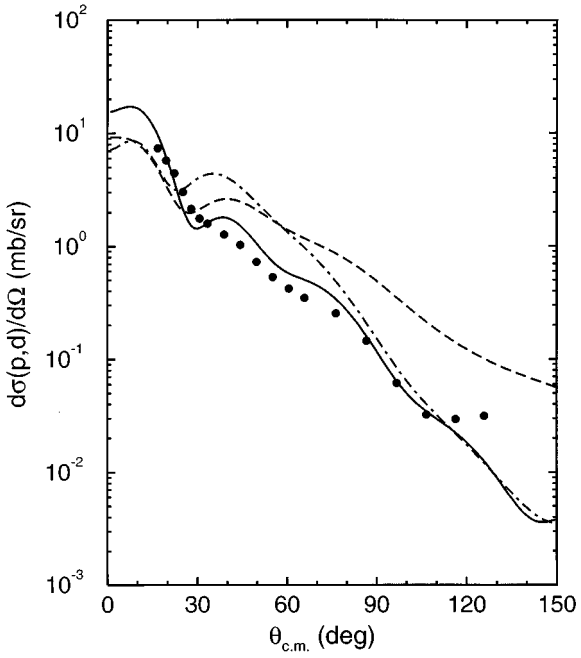

FIG. 2. Tabulated and calculated differential cross section angular distributions for the $^{13}C(p,d)^{12}C(g.s)$ reaction at 35 MeV. The figure compares the adiabatic (solid curve) and DWBA calculations using a deuteron folded (dot-dashed curve) and optical (dashed curve) potentials. The spectroscopic factor is 1.0 for all calculations.

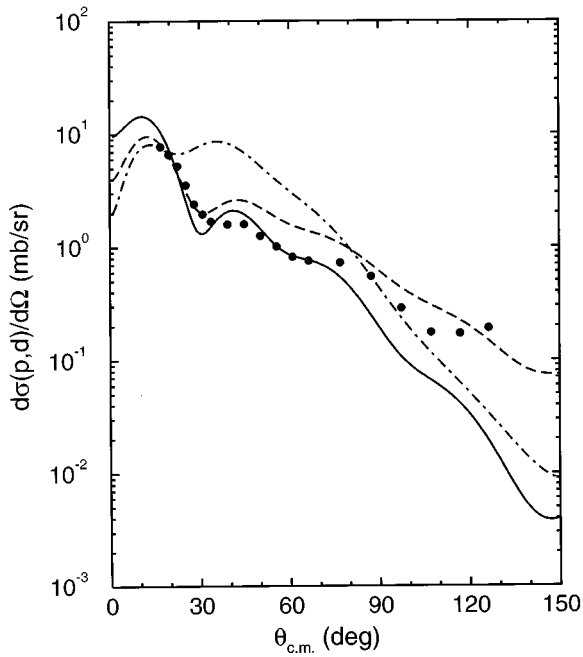

FIG. 3. Tabulated and calculated differential cross section angular distributions for the $^{13}C(p,d)^{12}C(2^+, 4.44$ MeV) reaction at 35 MeV. The curves are as in Fig. 2. The spectroscopic factors are 1.50, 1.60, and 1.12 for the adiabatic, DWBA (folding potential), and DWBA (optical potential) calculations, respectively.

A. (p,d) reaction calculations

We first calculate the $^{13}C(p,d)$ ^{12}C transitions in the adiabatic approximation and DWBA. These adiabatic (p,d) calculations determine the spectroscopic factors for the ground and 2^+ transfers which are then held fixed in the remaining calculations for the (p,d^*) reactions. We assume that the np interaction is the Hulthen potential of Ref. [18] for which $D_0(p,d) = -125.0$ MeV fm$^{3/2}$. Figure 2 shows the calculations and data [10] for the ground state $p_{1/2}$ neutron transfer. The solid curve shows the adiabatic model calculation. The dashed and dot-dashed curves are DWBA calculations assuming the Perey deuteron optical potential and folded deuteron potential (assuming the Bechetti-Greenlees [20] nucleon interactions), respectively. The calculated angular distributions are very similar to those of Toyokawa *et al.* [7] calculated within the coupled channels (CCBA and CDCC) description. The angular structure of the adiabatic three-body calculations provides a better description of the measurements. For this ground state transition, all calculations correspond to a spectroscopic factor of 1.0, which is the value subsequently assumed.

Figure 3 shows the calculations and data for the $p_{3/2}$ neutron transfer leading to the ^{12}C 2^+ final state. The curves are as in Fig. 2. The adiabatic calculation (solid curve) assumes a spectroscopic factor of 1.50, which is then held fixed. The breakup effects are large and DWBA calculations do not lead to a fast enough falloff with angle when compared with the empirical angular distributions. Our use of the zero-range approximation means that the absolute values of the spectroscopic factors obtained are slightly larger than those of the finite-range calculations of [7]. The ratio of the $p_{1/2}$ and $p_{3/2}$ spectroscopic factors is, however, very similar to that reported in this earlier analysis.

B. (p,d^*) reaction calculations

We now compare full adiabatic calculations of the $[p,d^*(S)]$ process against the tabulated singlet channel single differential cross section angular distributions [10]. Outgoing d^* c.m. angular distributions for the ground state and 4.44 MeV state transitions are calculated from Eq. (28) using the spectroscopic factors deduced from the (p,d) system. The full ε_r dependence in the integrand in the differential cross section is included in these calculations. The entrance and exit channel interactions are the same as those used for the (p,d) calculations.

The recently reported experiment [7] extracts only the $S=0$ channel angular distributions. The details of the analysis of the experiment are such that the tabulated $[p,d^*(S=0)]$ cross sections [10] correspond, in the language of this paper, to a value $\varepsilon_r^{\max}=1.0$ MeV [22]. In Figs. 4 and 6 we show the tabulated data points for the (p,d) (open circles) and $[p,d^*(S=0)]$ (solid circles) processes for the ground and 2^+ ^{12}C transitions, respectively. These figures show that the tabulated data for the ground and 2^+ states differ by a factor of less than an order of magnitude at forward angles, and that some $d^*(S=0)$ cross section data points actually exceed those of the (p,d) channel at larger angles. The ratio is of order 5, reaching a maximum of 8 in the diffraction minimum at 28°, for the $p_{1/2}$ transition and is of order 4 for the $p_{3/2}$ transition at 33°. Our adiabatic model estimate, for this $\varepsilon_r^{\max}$, was a factor of 37 difference in these cross sections.

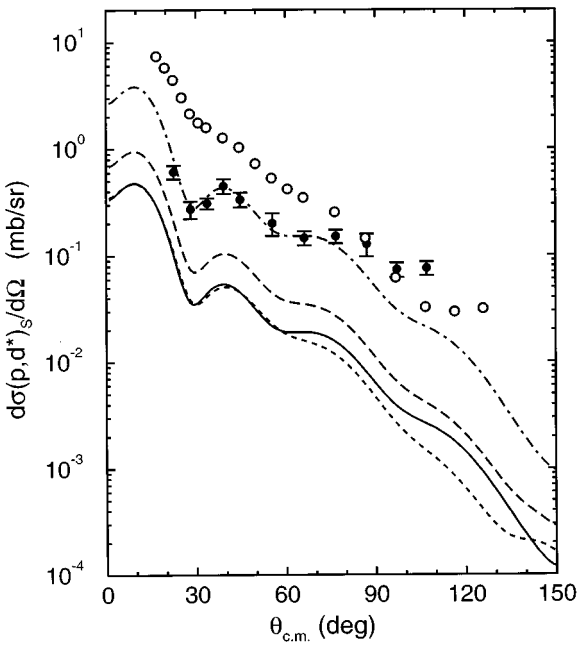

FIG. 4. Tabulated differential cross section angular distributionss for the $^{13}C(p,d)^{12}C(g.s)$ (open circles) and $^{13}C[p,d^*(S=0)]^{12}C(g.s)$ (solid circles) reactions at 35 MeV. The calculated singlet (solid curve), triplet (short dashed curve), and summed (long dashed curve) $[p,d^*(S)]$ contributions are also shown. The dot-dashed curve is 8 times the calculated $[p,d^*(S=0)]$ contribution.

The curves show the calculated singlet (solid curves) and triplet (short dashed curves) (p,d^*) contributions. The long dashed curves show the sum of these singlet and triplet contributions, which, as discussed in our earlier estimates, are approximately equal when integrated on the energy interval $0 \leqslant \varepsilon_r \leqslant 1.0$ MeV. Figures 5 and 7 show the calculated vector analyzing powers $iT_{11}(S)$ for the ground and 2^+ states. As in Figs. 4 and 6 the curves show the singlet (solid) and triplet (short dashed) (p,d^*) contributions. These are calculated from the $iT_{11}(S,\varepsilon_r)$ at each relative energy by averaging with respect to the double differential cross section of Eq. (27). The long dashed curves show the appropriately weighted summed contribution if one makes no spin separation in the final state. It is apparent that, for the ground state transition, this additional observable shows considerable sen-

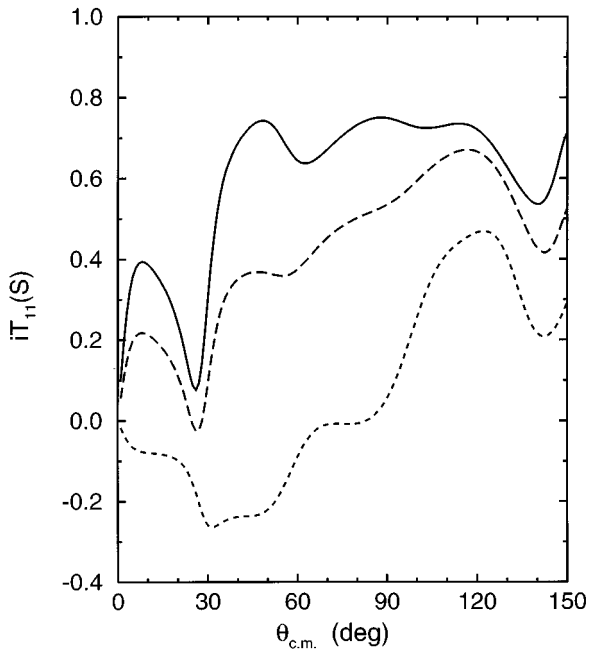

FIG. 5. Calculated vector analyzing power angular distributions for the $^{13}C[p,d^*(S)]^{12}C(g.s)$ reactions at 35 MeV. The calculated singlet (solid curve), triplet (short dashed curve) and summed (long dashed curve) $[p,d^*(S)]$ contributions are shown.

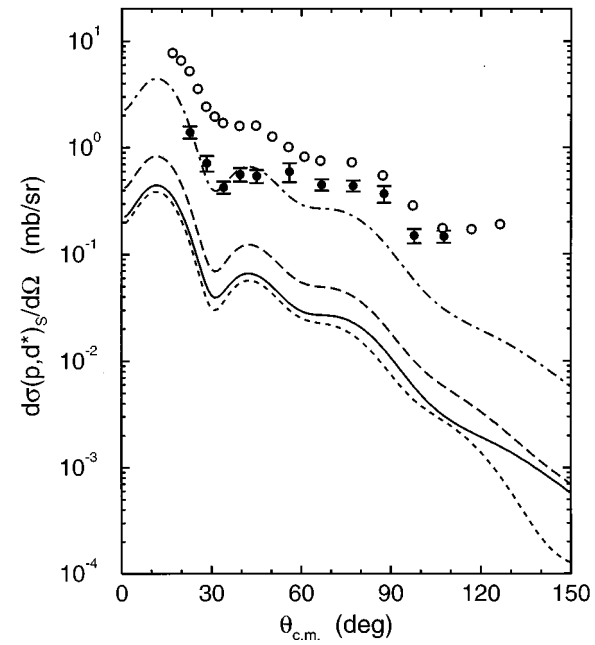

FIG. 6. As for Fig. 4, but for the $^{12}C(2^+, 4.44$ MeV) state transition at 35 MeV. The dot-dashed curve is now 10 times the calculated $[p,d^*(S=0)]$ contribution.

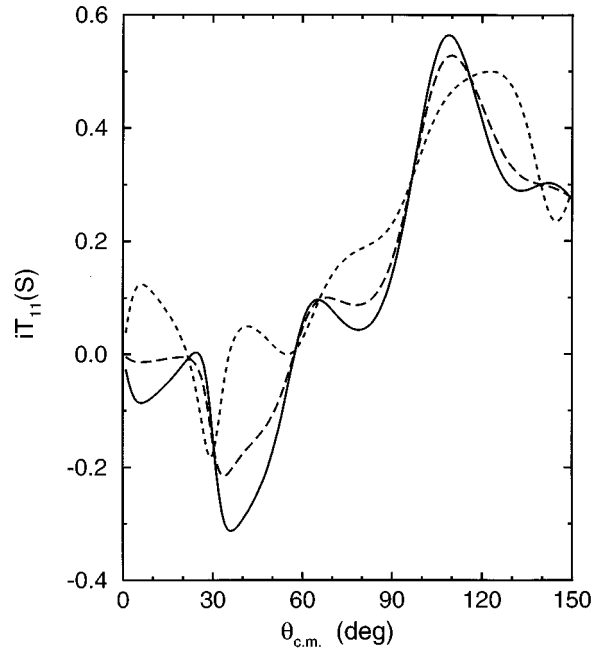

FIG. 7. As for Fig. 5, but for the $^{12}C(2^+, 4.44$ MeV) state transition at 35 MeV.

sitivity to the spin value of the continuum final states. (p,d^*) data using polarized protons would thus be of great value in clarifying these $S=0$ and $S=1$ continuum channel effects and the separation of data for the two channels.

There is clearly significant disagreement between the magnitudes of the adiabatic calculations of the singlet channel cross sections and the tabulated numbers and (CCBA and CDCC) calculations of [7] by almost an order of magnitude. To clarify the actual factor, the dash-dotted curves the Figs. 4 and 6 are obtained when the calculated singlet channel cross sections are multiplied by a factor of 8 for the ground state case, Fig. 4, and 10 for the 2^+ state, Fig. 6. These required renormalization factors indicate that our earlier estimate of a factor of order 37 difference in the cross sections is also confirmed by the full calculations which include the final state spin-dependent distortions and energy dependence.

C. Angular distributions

In addition to the observed differences in magnitude, the measured $[p,d^*(S=0)]$ cross sections fall off more slowly than the (p,d) cross section at large angles. The discussion of Sec. III suggested that the angular distributions for the (p,d) and both $[p,d^*(S)]$ channels should be rather similar if $E_f \approx \widetilde{E}_f$, provided the final state spin dependence is not large. In the full adiabatic calculations, the angular distributions for the singlet and triplet continuum are slightly different, the effect of correctly including the reaction Q values, and the spin-orbit interaction effects in the $S=1$ final state. The Q values are $-4.94-\varepsilon_r$ MeV in the (p,d^*) reactions and -2.78 MeV in the (p,d) reaction to the ^{12}C ground state. To clarify the importance of these effects, we rescale the full (p,d) and $[p,d^*(S=0)]$ cross section calculations to remove the transfer strength factors $(2S+1)D_0^2(p,d)$ and $\overline{D_0^2}(S=0,\varepsilon_r^{\max})$. That is, we evaluate

$$\frac{d\sigma(p,d^*)_{S=0}}{d\Omega_f} \Big/ \overline{D_0^2}(S=0,\varepsilon_r^{\max}) \approx \frac{\mu_i\mu_f}{(2\pi\hbar^2)^2}\frac{\overline{k_f}}{k_i}|M_{\rm ad}^{S=0}(\overline{\varepsilon_r})|^2 \tag{34}$$

and

$$\frac{d\sigma(p,d)}{d\Omega_f}/(2S+1)D_0^2(p,d) = \frac{\mu_i\mu_f}{(2\pi\hbar^2)^2}\frac{\widetilde{k}_f}{k_i}|M_{\rm ad}(p,d)|^2, \tag{35}$$

which would be equal in the absence of these considerations. The scaled angular distributions are shown in Fig. 8 by the solid (d) and dashed $[d^*(S=0)]$ curves. Thus, although the magnitudes of the $[p,d^*(S=0)]$ cross sections scale principally with $\overline{D_0^2}(S=0,\varepsilon_r^{\max})$, there are significant effects on the angular distribution due to the spin dependence and Q value effects. The magnitude of these effects is in reasonable accordance with the data, Figs. 4 and 6.

D. Comparison with CCBA and CDCC calculations

Coupled channels Born approximation calculations, which made use of the CDCC method [8] for treating the final states, accompanied the published data discussed above [7]. These CCBA calculations are discussed in more detail in Ref. [10]. Those calculations reproduced the magnitude of the tabulated $[p,d^*(S=0)]$ cross sections and thus also disagree with the calculations of the present work by approximately an order of magnitude. The CDCC calculations use a quite different technique for solving the three-body final state, reducing its description to an effective two-body coupled channels problem, with associated two-body phase space. The data are compared there with the calculated cross sections for transfer into a single np continuum bin state, constructed from np singlet states on the interval $0 \leq \varepsilon_r \leq 1.0$ MeV. Thus, while the calculations assume $\varepsilon_r^{\max}=1$ MeV, as used here, a single representative np breakup state is assumed, the simple average of the energy-dependent np scattering states over the 1.0 MeV interval.

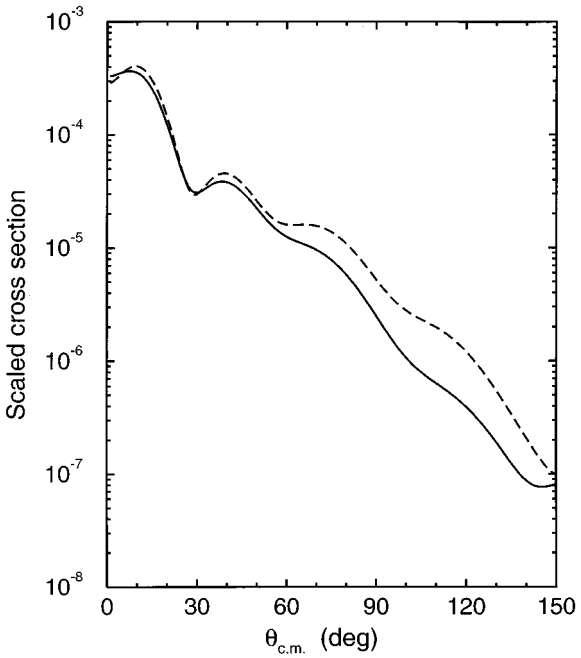

FIG. 8. Calculated (p,d) (solid curve) and $[p,d^*(S=0)]$ (dashed curve) cross section angular distributions for the ^{12}C(g.s) transition rescaled to remove the transfer strength factors $3D_0^2(p,d)$ and $\overline{D_0^2}(S=0,\varepsilon_r^{\max})$, respectively.

Additionally [10], when calculating the cross section angular distributions for the continuum transfers from the theoretical CCBA amplitudes, these amplitudes are multiplied by a Watson-Migdal-type multiplicative factor. Following usual notations, e.g., [23], this is denoted $1/|f(-\overline{k_r})|$ and, in [10], is evaluated at a representative np relative momentum. This factor will indeed enhance the calculated cross sections considerably. However, it is our understanding that the CDCC theory, as used by Toyokawa *et al.*, which uses realistic correlated and energy-dependent np scattering states in constructing the np relative motion bin states, already incorporates such final state interaction effects implicitly. Such three-body effects will therefore already have been included within the calculated CDCC and CCBA transition amplitudes.

In the adiabatic limit, discussed here, the double differential cross section is of course calculated for each final state relative np energy ε_r and the three-body phase space is retained. Such questions, relating to the treatment of the energy dependence of the np system, do not therefore arise.

V. CONCLUSIONS

Theoretical techniques for the treatment of transfer reactions leading to final states in the continuum, and to systems exhibiting virtual states, are likely to become increasingly important in our efforts to understand the structure of light nuclei at the neutron drip line. Given the limited accuracy, at present, of data for such exotic systems, the availability of high-precision light-ion data offers the opportunity to make quantitative investigations of the accuracy of theoretical models. The (p,d^*) reaction is particularly suited to study such effects, given that the system is described by the underlying free np interaction. The existence, in this case, of the bound deuteron system adds the requirement for a consistent description of both the bound and continuum transfers, and for the calculation of the correct relative strengths of the two processes.

To this end we have developed the adiabatic model formalism for (p,d^*) pickup reactions. We have applied the formalism to calculations of the $^{13}\mathrm{C}[p,d^*(S)]^{12}\mathrm{C}$ reaction with 35 MeV incident proton energy. The adiabatic approach is shown to make very clear the relationship between the three-body dynamics in the bound (p,d) and continuum (p,d^*) final states. For small values of the maximum detected relative energy of the np pair, $\varepsilon_r^{\max}$, the relative energy dependence of the (p,d^*) cross sections is determined principally by the intrinsic behavior of the free np system in singlet and triplet states. These singlet and triplet state contributions can be analyzed separately, due to the weak coupling between spin channels, at the energies of current interest. The contribution from the spin singlet state is dominant at small relative energies. By use of approximate and full adiabatic calculations, we calculate theoretical expectations for the singlet channel pickup cross section, relative to that of the (p,d) channel.

The calculated (p,d) and $[p,d^*(S=0)]$ cross sections are compared with recently reported experimental results. There is, approximately, an order of magnitude discrepancy between the calculated and reported singlet channel cross sections. By contrast, the (d,p) cross sections, which the adiabatic model shows are theoretically very closely related, are reasonably described both in magnitude and angular form.

Calculations of the vector analyzing power show that for the $^{13}\mathrm{C}[p,d^*(S)]^{12}\mathrm{C}$(g.s) transitions, the observable reveals considerable sensitivity to the channel spin value in the continuum final states. Additional (p,d^*) data using polarized proton beams would thus be of great value in clarifying this situation and quantifying the importance, and the separation of data, for the $S=0$ and $S=1$ channels. The presented adiabatic approach, for transfer reactions with three-body final states experiencing large final state interaction effects, is more generally applicable.

ACKNOWLEDGMENTS

The financial support of the United Kingdom Engineering and Physical Sciences Research Council (EPSRC) in the form of Grants Nos. GR/J95867 and GR/K33026 (for J.A.T.) and support by the Turkish Government (B.G.) are acknowledged. We acknowledge a number of extremely valuable discussions with Professor R.C. Johnson, and similarly with Professor H. Ohnuma and Dr. H. Toyokawa concerning details of the analysis of their experiment. The financial contribution of the British Council in support of these latter discussions is gratefully acknowledged.

[1] I.J. Thompson and M.V. Zhukov, Phys. Rev. C **49**, 1904 (1994).
[2] I. Slaus, Rev. Mod. Phys. **39**, 575 (1967).
[3] G. Temmer, Bull. Am. Phys. Soc. **9**, 108 (1964).
[4] M. Nomoto, Nucl. Phys. **81**, 180 (1966).
[5] K. Kolltveit and K. Nagatani, Nucl. Phys. **A124**, 287 (1969), and references therein.
[6] B.L. Cohen, E.C. May, and T.M. O'Keefe, Phys. Rev. Lett. **18**, 962 (1967); B.L. Cohen, E.C. May, T.M. O'Keefe, and C.L. Fink, Phys. Rev. **179**, 962 (1968).
[7] H. Toyokawa, H. Ohnuma, Y. Tajima, T. Niizeki, Y. Honjo, S. Tomita, K. Ohkushi, M.H. Tanaka, S. Kubono, and M. Yosoi, Phys. Rev. C **51**, 2592 (1995).
[8] M. Kamimura, M. Yahiro, Y. Iseri, H. Kameyama, Y. Sakuragi, and M. Kawai, Prog. Theor. Phys. Suppl. **89**, 1 (1986); N. Austern, Y. Iseri, M. Kamimura, M. Kawai, G. Rawitscher, and M. Yahiro, Phys. Rep. **154**, 125 (1987).
[9] R.C. Johnson and P.J.R. Soper, Phys. Rev. C **1**, 976 (1970).
[10] H. Toyokawa, Ph.D. thesis, RCNP, Osaka University report, 1995.
[11] J.D. Harvey and R.C. Johnson, J. Phys. A **7**, 2017 (1974).
[12] J.S. Al-Khalili, J.A. Tostevin, and R.C. Johnson, Nucl. Phys. **A514**, 649 (1990).
[13] M. Yahiro, J.A. Tostevin, and R.C. Johnson, Phys. Rev. Lett. **62**, 133 (1989).
[14] G.G. Ohlson, Nucl. Instrum. Methods **37**, 240 (1965).
[15] E.J. Stephenson, A.D. Bacher, G.P.A. Berg, V.R. Cupps, C.C. Foster, N. Hodiwalla, P.C. Li, J. Lisantti, D.A. Low, D.W. Miller, C. Olmer, A.K. Opper, B.K. Park, R. Sawafta, S.W. Wissink, J.A. Tostevin, D.A. Coley, and R.C. Johnson, Phys. Rev. C **42**, 2562 (1990).
[16] R.V. Reid, Ann. Phys. (N.Y.) **50**, 411 (1968).
[17] V.G.J. Stoks, R.A.M. Klomp, C.P.F. Terheggen, and J.J. de Swart, Phys. Rev. C **49**, 2950 (1994).
[18] A. Laid, J.A. Tostevin, and R.C. Johnson, Phys. Rev. C **48**, 1307 (1993).
[19] M. Igarashi, M. Toyoma, and N. Kishida, computer program TWOFNR (private communication).
[20] F.D. Bechetti and G.W. Greenlees, Phys. Rev. **182**, 1190 (1969).
[21] C.M. Perey and F.G. Perey, At. Data Nucl. Data Tables **17**, 1 (1976).
[22] The CDCC calculations, which describe the final state in the CCBA calculations of [7], are discussed in more detail in Ref. [10]. The data are compared there with the cross section for transfer to a single np continuum bin state, constructed from np singlet states on the interval $0 \leqslant \varepsilon_r \leqslant 1.0$ MeV.
[23] U. Janetzki, Q.K.K. Liu, D. Hahn, H. Homeyer, and J. Scheer, Nucl. Phys. **A267**, 285 (1976).